TÉCNICO LISBOA

Ultrasonic tomography in the evaluation of fire-induced damage on a Portuguese limestone

Mauro João Ebondo Batista Amaral

December, 2020.

A B S T R A C T

The effect of high temperatures on natural stone is an important factor that contributes significantly to its degradation. The increase in temperature promotes changes in the internal structure of the stone, resulting in variations in its chemical, physical and mechanical properties. The aim of this dissertation was to study some of the important physical changes, due to the thermal effect, on a Portuguese limestone: the white-cream variety of the Ançã Limestone. For this purpose, a multianalytical approach combining ultrasonic tomography with physical properties (capillary absorption coefficient, open porosity and apparent density) and with elastic parameters (VP, VS, VP/VS, E, K, μ and ν) has been applied to characterize the degradation processes induced by high temperatures. The samples were tested at room temperature (reference samples), at 300ºC, and 600ºC under different cooling conditions (partial or total immersion in water at room temperature). The capillary absorption coefficient and open porosity increased with increasing temperature while the elastic constants, with exception of the Poisson's ratio, decreased. The variations in the studied properties were different for different cooling situations. In fully immersed samples, mechanical degradation was more pronounced compared to partially immersed samples. Through the obtained ultrasonic tomograms, it was possible to observe the distribution of the P-waves velocity and to identify the areas most affected by the high temperatures. With the increase in temperature, it was also possible to observe a significant increase in the VP anisotropy index, resulting in an increase in heterogeneity in the distribution of the P-waves velocity.

Keywords: White-cream Ançã Limestone; Ultrasonic Tomography; Thermal Decay; Physical Parameters; Elastic Parameters; P and S-waves velocity.

1. Introduction

Natural stone occupies an important place in Society due to its widely use both in construction and at the ornamental level throughout the History. Therefore, it is necessary to identify its decay agents in order to promote its conservation and preservation. Among the natural or anthropic factors, which have gained preponderance in recent years, is the effect of the high temperatures reached during fires. Large-scale fires are increasingly common in Portugal and worldwide. Most of the time, these events have destructive effects, not only in forested areas but also on a social level, with the destruction of residential, business, industrial, and cultural buildings.

The total or partial destruction of buildings by fires, including large monuments is of great concern to the European Community. Indeed, the research report recognized at the supranational level (COST Action C17) estimates that in Europe, one historic building is lost each day due to fires [1].

The study of the effect of fires on natural stone is of high importance since high temperatures affect its chemical, physical and mechanical properties. The first studies on stone fire effect were based on macroscopic observations carried out in situ and included macroscopic observation of different forms of degradation such as chromatic changes, granular disintegration, and cracking [2]. Currently, the approach is diverse and includes studies that analyse changes in different properties such as porosity, texture, mineralogical composition, capillarity, permeability [3]–[5]. Furthermore, several researchers based their study on the variations in mechanical and physical properties such as, for example, the P-wave and S-wave velocity, Young's modulus, density, uniaxial and flexural strength e.g. [3], [6]–[8].

When stone is heated during a fire, a temperature gradient is generated from the surface to the inner part of the stone, due to the temperature difference, which promotes mineral linear and volumetric expansions. As a result, creation of microcracks, fractures, exfoliation, granular disintegration, flaking and, in some cases, depending on the mineralogical composition, discoloration are observed [9]. These changes imply variations in the chemical, physical and mechanical properties of the stone, whose intensity varies according to their intrinsic characteristics, as well as the characteristics of the fire (temperature, duration, extinction form, etc.).

The current study intended to measure the transit time of longitudinal waves, by non-destructive method, to build a 3D velocity distribution model based on tomographic inversion. With the 3D elastic velocity model (for reference

and artificially heated samples) comparisons were made in order to evaluate the decay due to the exposure to high temperatures [10].

2. Materials and methods

2.1. Stone material

The white-cream variety of the Portuguese Ançã limestone was selected for this study based on its widespread use in Portuguese architectural and sculptural monuments in Coimbra area due, not only to its geological occurrence, but specially to its beauty and workability.

This stone can be described as being a compact limestone varying its color between white, white-cream, and more or less dark gray. With a relatively high porosity, this limestone is very vulnerable to the salt crystallization. Thus, cases of very significant loss of exposed material's surfaces are frequent, sometimes reaching dramatic degrees of material's loss and, consequently, of their historical and aesthetic significance [11]. A detailed geological context, petrography, mineralogy and physical-mechanical properties of this limestone is presented by Quinta-Ferreira et al. [12].

Stone samples were obtained from an old quarry from Arocal (Coimbra) and latter cut into parallelepiped probes with a 5 cm x 12 cm x 5 cm (width x length x height) using a diamond saw. Six samples were used for the laboratory experiments and identified from 1 to 6. Their faces were identified as Face A, Face L, and Face AA (each face corresponds to a direction) and, a regular mesh spaced by 5 mm x 5 mm was marked on all the faces of the samples, totaling 550 points per sample (Fig. 1). This marking was essential to assess changes in the transit time of P-waves, before and after samples were subjected to high temperatures.

2.2. Laboratorial heating procedure

In the laboratorial tests, two heating temperatures were considered: 300ºC and 600ºC, using an electric muffle Naberthem (Program Controller S27) with a heating rate of 10ºC/min (choose based on published works to replicate heating rates that occur in real cases [13]). After reaching each of the desired temperatures, the samples were kept at those conditions for 2 hours to ensure a uniform temperature distribution within the stone.

Since fire extinguishing of is usually carried out using cold water promoting additional thermal shocks on the surfaces affected by high temperatures, an attempt was made to replicate this effect after the heating phase. Thus, the samples were immediately removed from the muffle after the exposure time to 300ºC or 600ºC and divided into two sets for each temperature threshold, that is, their rapid cooling was promoted under different conditions: (i) total immersion (sample was completely submerged in water at room temperature, for 30 seconds); and (ii) partial immersion of the samples (only one centimeter of face A was immersed) in the water at room temperature, for 30 seconds.

2.3. Testing methods

Several parameters were evaluated before and after heating such as water absorption by capillarity, open porosity, apparent density, P and S-wave velocities, and dynamic elastic modulus. Moreover, macroscopic (visual appearance) features were also evaluated.

2.3.1. Water absorption by capillarity

The water absorption by capillarity test was performed based on the experimental procedure described in the European standard EN 1925:1999 [14], which applies to natural stone.

The test was carried out in two perpendicular directions for each reference sample. For samples 1, 2, 3, and 4 the tests were performed according to the directions of faces A and AA and, for samples 5 and 6, the tests were performed according to the directions of faces A and L. After being heated and, taking into account results obtained from the P-waves velocities, it was necessary to assess the capillarity test for the 3 directions considered in each sample.

2.3.2. Open porosity and apparent density

The open porosity and apparent density test were performed based on the European standard EN 1936:2006 [15].

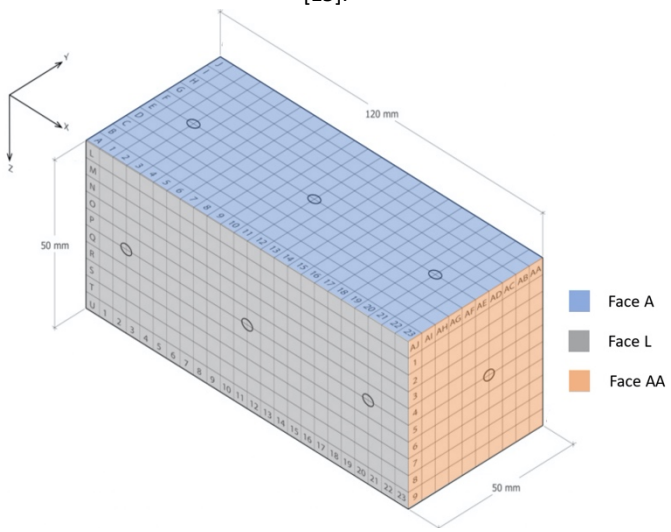

Figure 1 - Layout of the ultrasonic propagation velocity directions measured in the specimens and measurement points of P and S-w

2.3.3. Ultrasonic measurements

The measurement of the travel times of the P-waves was performed using the Steinkamp Ultrasonic Tester BP-7 equipment. The transmission method was used, i.e., two piezoelectric sensors were coupled on opposite faces of the specimen and the transit time for the ultrasonic pulse travelling through two opposite positions was measured. The point-contact transducers (a transmitter and a receiver) used have resonance frequency of 45 kHz, with measuring range from 0.1 μs to 9999.9 μs and accuracy of 0.1 μs. A viscoelastic couplant was placed to ensure a good contact between the transducers and the stone specimen's face. The P-wave travel time was measured following a grid with 5.0 mm x 5.0 mm, with a total of 550 transmitter-receiver pairs (Fig. 1).

The first step in creating the seismic velocity models involves the tomographic inversion of the times of the first arrivals of the seismic waves. The inversion method, developed by Mendes [16], is based on the Simultaneous Iterative Reconstruction Technique (SIRT) and requires prior knowledge of the medium velocity to build an adequate initial model. The requirement for an initial velocity model that is relatively close to the final velocity model, allows the inversion algorithm to have a good convergence. The 3D inversion started, for simplicity, with a constant velocity model. The interactive process stopped when the root-mean-square (RMS) error reached the accuracy of the measurements (less than 0.2 microseconds).

In order to calculate the elastic constants: Young's modulus (E); shear modulus (μ), bulk modulus (K) and Poisson's ratio (ν) for the different test conditions, P and S waves were measured at 7 points of each sample (Fig. 1). The measurement was performed using the HMO 1002 Series oscilloscope from ROHDE & SCHWARZ with 2 horizontally polarized transducers. Through the wave observed on the oscilloscope, the travel times of the P and S-waves were identified.

2.3.4. Anisotropic evaluation

The anisotropy of the samples was calculated according to the index proposed by Birch [17]. Usually, it's determined by measuring the propagation velocity of the P-waves in different directions of the stone. However, in this study, the anisotropy index was adapted and also calculated according to the capillary coefficient measured in the 3 directions of the samples under analysis.

3. Results

3.1. Macroscopic observations

After the heating and cooling cycle to which the samples were exposed, only chromatic changes were observed at the macroscopic level (Fig. 2). When heated at 300ºC, the samples changed from white-cream to shades of cream-beige colour. For the temperature of 600ºC, the samples became even darker taking shades of dark grey.

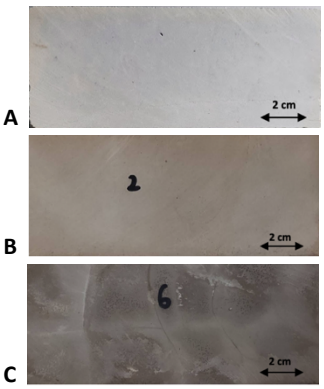

Figure 2 - Detail of the chromatic changes of the tested samples with the increase of temperature: (A) At room temperature; (B) Heated et 300ºC; (C) Heated at 600ºC.

3.2. Physical quantification

Table 1 summarizes the results obtained in the different test phases, in terms of water capillary absorption coefficient, open porosity and apparent density.

3.2.1. Water absorption by capillarity

The results presented in Table 1, indicate that the capillary absorption coefficient increases with increasing temperature, with a more evident increase for samples heated to 600ºC. Samples heated at 300ºC show an average increase in the capillary absorption coefficient of 18%, 11%, and 8% for samples 1, 2, and 3, respectively. For samples heated at 600ºC, an average increase in the capillary absorption coefficient of 39%, 42%, and 69% is observed for samples 4, 5, and 6, respectively. It should be noted that partial immersion for samples 2, 3, and 6 was carried out on the face called Face A. In samples heated to 600ºC, it is shown that the sample partially cooled in water (sample 6) has a higher growth rate (in mean terms) of the capillary absorption coefficient when compared with samples 4 and 5 that were fully immersed. The same was not observed in samples heated to 300ºC. For this temperature, the sample fully immersed (sample 1) presents, approximately, the highest growth rate of the capillary coefficient when compared with the samples partially immersed (samples 2 and 3). It should also be noted that the Face AA shows a smaller increase in the capillary absorption coefficient compared to the Face A in the case of samples 1, 2, 3, and 4 and with the Face L in the case of samples 5 and 6. Contrary to what was observed for all samples, the capillary absorption coefficient decreased by about 13% on the Face AA face of sample 3.

From the capillary absorption coefficient of the heated samples, the anisotropy index (k), proposed by Birch [17], was calculated. The results of the anisotropy index are as follow: 0,17; 0,12; and 0,79 for the samples 1, 2 and 3, respectively and 0,46; 0,52 and 1,00 for the samples 4, 5 and 6, respectively. Sample 3 has a higher anisotropy index compared to other samples heated to 300ºC and, among samples heated to 600ºC, sample 6 is the one with the highest anisotropy index. It can also be stated that, given the values of the capillary coefficients (table 1), the most anisotropic directions or faces are: i) Face A for samples 3, 4, and 6; ii); Face L for samples 2 and iii) Face AA for samples 1 and 5.

The evaluation of the effect of cooling on partially immersed samples can be made by comparing the values of

the absorption coefficients between face A and its opposite face (not immersed). For this, the capillary test was repeated on the opposite side to the one that was initially immersed (Fig. 3). Indeed, capillarity water absorption coefficient is slightly higher when the test is performed on the face immersed in water and this difference is more pronounced in sample 6 (heated to 600ºC).

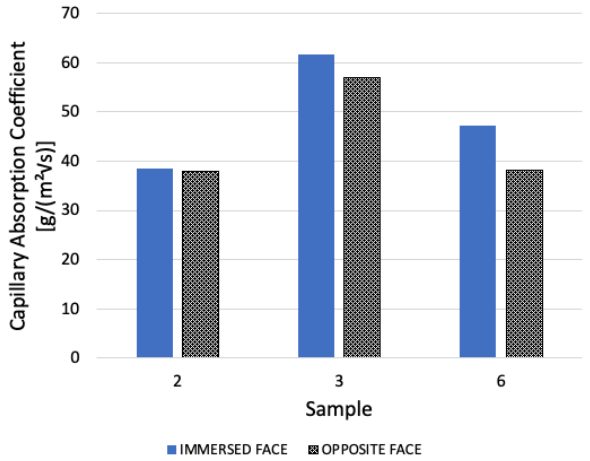

Figure 3 - Comparison of capillarity coefficients between opposite faces in partially immersed samples.

3.2.2. *Open porosity and apparent density*

Open porosity increased with increasing temperature, being more pronounced for samples heated to 600ºC (Table 1). The cooling method (total and partial immersion in water) also caused changes in open porosity. For samples heated to 300ºC, the sample 1 (fully immersed) shows greater growth in open porosity (12%) when compared to the values obtained of samples 2 (5%) and 3 (9%). The same trend is verified when the values of open porosity for samples heated to 600ºC are analysed. Samples 4 and 5 (fully immersed) show greater growth in open porosity (27% and 33%, respectively) when compared to the value of sample 6 (21%) which was partially immersed.

Apparent density decreased slightly with increasing temperature (Table 1). For samples heated to 600ºC there was a reduction of 2.6%, 2.8%, and 3.3% (samples 4, 5 and 6, respectively) while for samples heated to 300ºC, the reduction was 0, 6%, 0.2%, and 0.4% (samples 1, 2 and 3, respectively). This decrease may be related to material loss. In fact, it has been observed that, for samples heated to 600ºC, the average reduction in mass values was 0.5%, 0.7%, and 0.6% for samples 4, 5, and 6, respectively. For samples heated to 300ºC, the reduction was 0.3%, 0.1%, and 0.3% for samples 1, 2, and 3, respectively.

3.2.3. *Ultrasonic measurements*

Table 2 shows the average values of P-waves velocity obtained for each face of the reference samples and after being heated at 300ºC (grey) and 600ºC (red). The results show that P-waves velocity decreased significantly with the increase in temperature. For samples heated at 300ºC an average reduction of 13% was observed while in samples heated to 600ºC the average reduction observed was 53%.

Table 1 - Petrophysical parameters for reference, heated at 300ºC and 600ºC samples. (TI - Total Immersion; PI - Partial Immersion; ND - Not Determined).

Parameters		Sample 1 (TI)		Sample 2 (PI)		Sample 3 (PI)		Sample 4 (TI)		Sample 5 (TI)		Sample 6 (PI)	
		REF.	300ºC	REF.	300ºC	REF.	300ºC	REF.	600ºC	REF.	600ºC	REF.	600ºC
Capillary Absorption Coefficient [(g/(m²√s)]	A	24,93	31,47	33,43	38,5	48,68	61,79	29,48	53,02	34,98	55,3	23,88	47,33
	L	ND	33,58	ND	35,39	ND	33,22	ND	40,21	36,8	46,65	20,93	28,26
	AA	25,68	28,35	37,6	40,08	41,83	36,26	33,75	34,71	ND	31,2	ND	19,03
Open Porosity (%)		10,72	12,02	12,1	12,69	13,85	15,16	12,03	15,24	11,87	15,83	10,86	13,16
Density (g/cm³)		2,61	2,60	2,53	2,52	2,42	2,41	2,50	2,49	2,52	2,50	2,52	2,51

Table 2 - Average values of the P-waves velocity and anisotropy index for the reference samples and after being heated to 300ºC (grey) and 600ºC (red).

Sample	Reference (m/s)			Heated (m/s)			Anisotropy	
	Face A	Face L	Face AA	Face A	Face L	Face AA	Reference	Heated
1 (TI)	4369	4169	4414	3703	3135	3284	5,6	17,3
2 (PI)	4186	4245	4145	3821	3578	3806	2,4	6,4
3 (PI)	4009	3714	4103	3878	3372	3788	9,7	13,4
4 (TI)	4069	4145	4221	2130	1508	932	3,7	79,4
5 (TI)	3978	4067	4072	1468	1963	1085	0,1	59,8
6 (PI)	4169	4180	4424	3250	1956	1615	6,1	83,6

To assess the anisotropy of each specimen, the anisotropy index (k), proposed by Birch (1961), was calculated (Table 2). Before heating, samples 2 and 5 had the lowest P-wave anisotropy, while samples 3 and 6 were those with the highest anisotropy. With increasing temperature, anisotropy also increased, being more pronounced for samples heated to 600ºC. However, it appears that the samples with the highest anisotropy index before heating are those that show the lowest growth in this index after heating. For samples heated to 300ºC (sample 1, 2 and 3), sample 3, which has a higher anisotropy index before being heated, shows an increase of 38%, when compared to samples 1 and 2, which showed a growth of 208% and 167%, respectively. For samples heated to 600ºC (samples 4, 5, and 6), sample 6, with a higher anisotropy index before heating, showed an increase in the anisotropy index of 1270%, when compared to samples 4 and 5, which showed an increase of 2070% and 42600%, respectively.

Similar to what was observed in the absorption of water by capillary, also regarding the P-wave velocities, it was observed that, in heated samples, the anisotropy of P-wave is lower in sample 2 and higher in sample 6. It was also possible to identify the most anisotropic direction for each heated sample. The most anisotropic directions of the heated samples are: i) face A for samples 1, 4, and 6, ii) face L for samples 2 and 3, and iii) face AA for sample 5.

The cooling method also appears to have an influence on the P-wave anisotropy index. The fully immersed samples show greater growth in the anisotropy index than those partially immersed.

The 3D inversion of P-wave first arrivals for the reference samples allowed to obtain, with the data of the 3 directions, their tomograms (figures 4A, 5A, 6A, 7, 8, and 9). However, due to the high anisotropy of the heated samples it was only possible to obtain tomograms, with data from the 3 directions, for the heated samples 2 and 3. For sample 1, the tomogram was obtained using data from the two less anisotropic directions (L and AA). For comparative purposes, the tomogram of the reference sample 1 obtained with data from the two less anisotropic directions is also presented (figure 4 B). The tomograms of the six reference samples are shown in figures 4A, 5A, 6A, 7, 8, and 9) and the tomograms of the samples heated to 300ºC (samples 1, 2, and 3), are shown in the figures 4C, 5B and 6B, respectively with three 2D sections obtained at x = 25 mm, x = 50 mm and x = 75 mm.

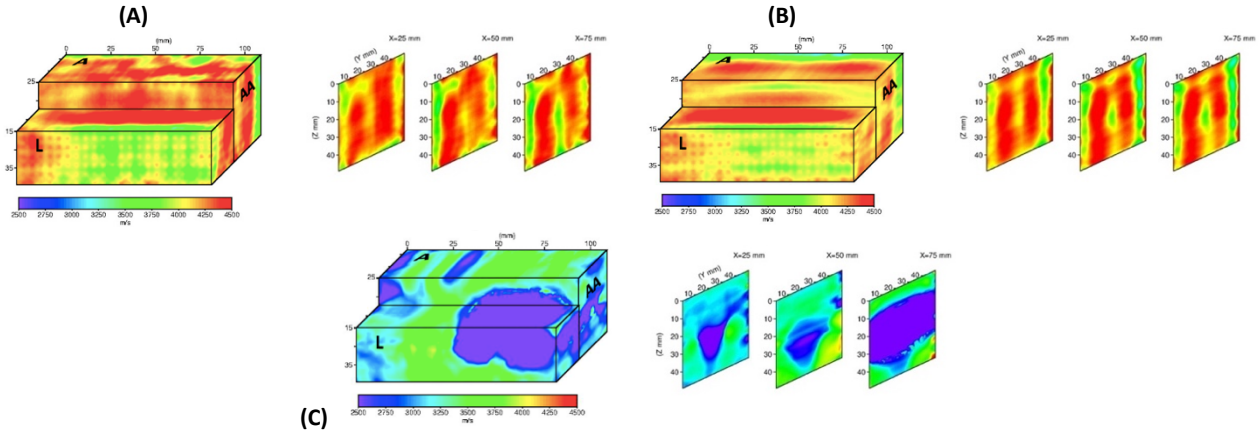

Figure 4 - 3D model with 2D sections (at x = 25, x = 50 and x = 75 mm) with the distribution of P-wave velocities for sample 1: before heated and obtained with the velocities in 3 directions (A); before heating and obtained with the velocities in 2 directions (B); after heating at 300ºC obtained with the velocities in 3 directions (C).

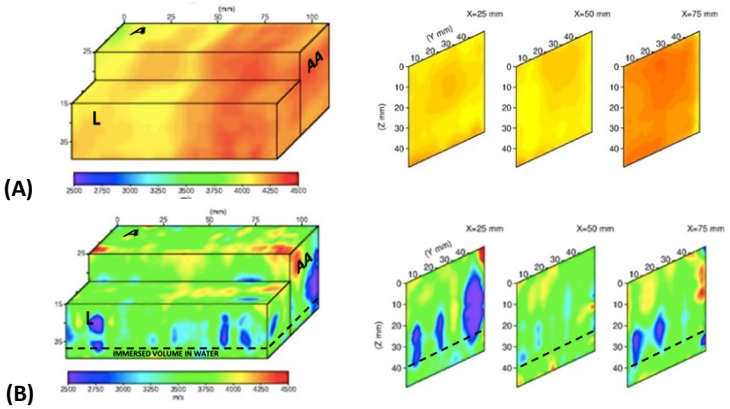

Figure 5 - 3D model with 2D sections (at x = 25, x = 50 and x = 75 mm) with the distribution of P-wave velocities for sample 2: before heated and obtained with the velocities in 3 directions (A); after heating to 300ºC obtained with the velocities in 3 directions (B).

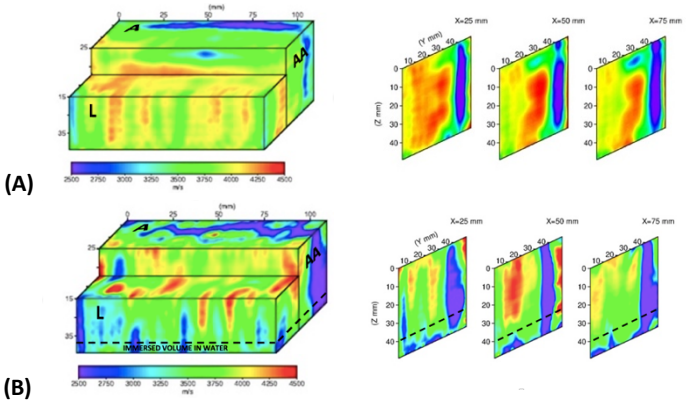

Figure 6 - 3D model with 2D sections (at x = 25, x = 50 and x = 75 mm) with the distribution of P-wave velocities for sample 3: before heated and obtained with the velocities in 3 directions (A); after heating to 300ºC obtained with the velocities in 3 directions (B).

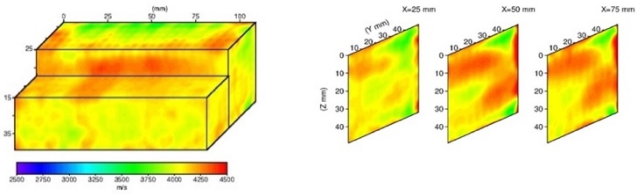

Figure 7 - 3D model with 2D sections (at x = 25, x = 50 and x = 75 mm) with the distribution of P-wave velocities for sample 4 before heated obtained with the velocities in 3 directions

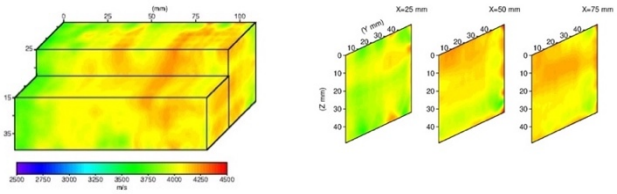

Figure 8 - 3D model with 2D sections (at x = 25, x = 50 and x = 75 mm) with the distribution of P-wave velocities for sample 5 before heated obtained with the velocities in 3 directions

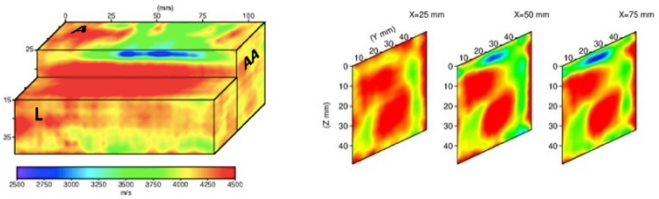

Figure 9 - 3D model with 2D sections (at x = 25, x = 50 and x = 75 mm) with the distribution of P-wave velocities for sample 6 before heated obtained with the velocities in 3 directions

The tomograms of the reference samples (figures 4A, 5A, 6A, 7, 8, and 9) shows that the samples 1, 2, 4, and 5 (figures 4A, 5A, 7 and 8, respectively) have a more homogeneous distribution of the P-wave velocity (3750-4250 m/s) whereas in samples 3 and 6 (figure 6A and 9, respectively) the distribution is more heterogeneous with extreme velocity values (2750 - 4500 m/s).

With the increase in temperature, the heterogeneity in the velocity distribution was also higher. Sample 1 (figure 4C) showed a distribution between 2500-3750 m/s while samples 2 and 3 (figures 5B and 6B, respectively) showed a distribution between 2500-4500 m/s. When heated, the samples underwent significant decreases in velocity values (approximately 1000 m/s for sample 1 and about 500 m/s for samples 2 and 3). This decrease was more accentuated in sample 1 (figure 4 C) where there are several areas of the sample where the velocity reaches minimum values (2500 m/s) while in samples 2 and 3 (figures 5B and 6B) the lowest values are only visible in some areas. In addition, it appears that the tomogram obtained with the data in 3 directions (figure 4A) does not differ significantly from the tomogram obtained with the data in the two less anisotropic directions (figure 4B).

3.2.4. Elastic parameters

From the P and S-waves velocities obtained through the travel times determined at 7 points of each sample (fig. 1), it was possible to calculate the elastic parameters. All those values (VP, VS, VP/VS, E, μ, K and v) are summarized in table 4.

The measurement of the travel time of the S-waves on the Face AA in samples 5 and 6 (heated at 600ºC) was not possible since the waves on the oscilloscope didn't had the characteristics required. Those values will be identified by ND (not determined).

Elastic parameters E, μ, and K decrease significantly with the increase in temperature (table 3). For samples heated at 300ºC, the average reduction in E was 65%, 50%, and 48% for samples 1, 2, and 3, respectively; while for samples heated to 600ºC the average reduction was 90%, 92%, and 87% for samples 4,5 and 6, respectively.

In the case of μ, for samples heated to 300ºC, the average reduction was 68%, 54%, and 53% for samples 1, 2, and 3, respectively. For samples heated to 600ºC, an average reduction of 91%, 92%, and 88% was observed for samples 4, 5, and 6, respectively.

Regarding K, there was an average decrease of 33% and 12% for samples 1 and 2, respectively, and an average increase of 12% for sample 3. For samples heated to 600ºC, an average decrease was observed was 72%, 77%, and 73% for samples 4, 5, and 6, respectively.

As for E, μ, and K, the Poisson's ratio was also calculated for the three directions, in the six samples tested. The increase in the Poisson's ratio is more significant for samples heated to 300ºC with an average increase of 48% (49%, 53%, and 41% for samples 1,2 and 3, respectively) compared to samples heated to 600ºC with an average increase of 29% (19%, 57% and 25% for samples 4,5 and 6, respectively). The reference samples had an average Poisson's ratio of 0,25. When heated at 300ºC, the value increased to 0,37. With the temperature raised up to 600ºC, the average value of the Poisson's ratio decreased to 0.35. However, sample 4, heated to 600ºC, had two values of the Poisson's ratio (0.17 and 0.16) very different from the values obtained in the other 5 points and in the other two samples heated up to 600ºC. These values may be related to the errors associated with the difficulty of measuring the travel time of the S-waves. If these two values are not considered when calculating the average values of the Poisson's ratio for heated samples, the average Poisson's ratio takes the value of 0.38. This increase means that samples heated to 600ºC show a greater increase in the Poisson's ratio compared to samples heated to 300ºC.

Table 3 - Physical and elastic parameters for the samples before (Blue) and after being heated (grey - 300ºC; red - 600ºC).

Parameters	Sample 1		Sample 2		Sample 3		Sample 4		Sample 5		Sample 6	
	Reference	300ºC	Reference	300ºC	Reference	300ºC	Reference	600ºC	Reference	600ºC	Reference	600ºC
VP (m/s)	4216,43	3000,99	4207,37	3527,43	4088,56	3745,77	4191,25	1632,98	4252,18	1656,02	4468,61	1919,18
VS (m/s)	2437,72	1360,91	2425,50	1622,83	2309,36	1582,92	2411,97	683,75	2369,80	636,71	2480,70	850,51
VP/VS	1,73	2,21	1,74	2,19	1,77	2,38	1,74	2,35	1,80	2,58	1,80	2,21
E (Gpa)	38,77	13,55	37,10	18,49	32,61	16,83	36,37	3,69	35,95	3,04	39,69	5,26
μ (Gpa)	15,53	4,95	14,88	6,80	12,93	6,10	14,55	1,35	14,15	1,08	15,55	1,92
K (Gpa)	25,76	17,35	24,94	22,78	23,34	26,10	24,55	6,75	26,66	6,01	29,71	7,95
Poisson's ratio (v)	0,25	0,37	0,25	0,37	0,26	0,38	0,25	0,33	0,27	0,40	0,28	0,35

4. Discussion

When the stone is subjected to high temperatures, a temperature gradient is initially created between the exposed surface and its interior, which favors linear and volumetric expansions that, in turn, promotes the development of fractures, microcracks and granular disintegration [9]. These changes in the internal structure of the stone are reflected in an increase in water absorption by capillary and an increase in open porosity. Through the capillarity and open porosity tests it was possible to observe the increase in the water absorption capacity by capillary and the open porosity with the increase in temperature. This observation is in agreement with the results obtained by several authors for limestone samples submitted to temperatures up to 800ºC [10],[18]–[20]. Martinho et al. [10], concluded that the increase in the water absorption capacity by capillarity is related to the increase of voids inside the rock resulting from the creation and development of pores and fissures (intergranular and/or intragranular), associated with the thermal expansion of the calcite crystals within the limestone samples which is known to have an anisotropic thermal expansion, i.e., the expansion is done in parallel and the contraction is made perpendicular to the crystallographic axis (c-axis).

The increase in open porosity is also related to the initial porosity of the rock, that is, before heated [21]–[24]. In fact, Gomez-Herras et al. [24] related the increase in the growth rate of open porosity, due to exposure to high temperatures, with the initial porosity of the material. These authors concluded that, in the samples with higher initial porosity, the rate of variation of the porosity with the temperature is lower in the less porous rocks. This conclusion may justify the observed fact where a greater increase of open porosity was observed in sample 1 (12%), with a lower initial porosity (10.72%), compared to the growth rates of samples 2 and 3 (3% and 9%, respectively) that have higher initial porosity values (12.10% and 13.85%, respectively). According to the authors of this study, a high initial porosity value indicates that there are larger empty spaces that can support the thermal expansion of mineral grains and, therefore, the variation in porosity is lower compared to rocks with low initial porosity. However, it is important to note that, in the case of the work developed in this thesis, the samples were subjected to different types of cooling (total and partial immersion in water). The results show that in samples heated at 600ºC, the growth rate of open porosity of sample 6 (21%), with lower initial porosity (10.86%), is lower when compared to the growth rate of samples 4 and 5 (27% and 33%, respectively) that have initial porosities of 12.03% and 11.87%, respectively. However, sample 6 was cooled by partial immersion in water while samples 4 and 5 were fully immersed, for the period of time. The fact that sample 6 is partially immersed in water at room temperature causes it to undergo minor changes in its porous network. This is due to the fact that a temperature gradient is established at only one face compared to samples 4 and 5 where a temperature gradient develops on all faces. This aspect is reflected in a smaller increase in open porosity. According to Brotons et al. [21], the increase in open porosity for samples cooled completely in water is due to the creation of microcracks that connect the

pores of the sample, whereas in samples cooled to room temperature, the increase in open porosity is due to the increasing in the quantity and size of pores. In contrast to open porosity, the water absorption capacity by capillary does not seem to be influenced by the type of immersion to which the samples were subjected, since there were no noticeable differences in the results. However, for samples partially immersed, it appears that the capillary coefficient is slightly higher on the water-immersed face compared to the opposite (not immersed) face. This behavior can be explained by the creation of larger amounts of voids that formed in the vicinity of the water-cooled face due to the greater thermal shock to which it was subjected when compared to its opposite face.

The decrease in apparent density is directly related to the increase in open porosity, but not proportionally. The decrease in density can also be related to the loss of mass that occurred with the increase in temperature. Sun et al. [3], Beck et al. [25] Zhang et al. [26] and Meng et al. [27] observed the same behavior in limestone samples that were heated to temperatures up to 900ºC. Meng et al. [27] found that the rate of material loss for samples heated to temperatures below 400ºC was only 0.18%. However, for temperatures between 400ºC and 500ºC, the loss was 0.21% and, for temperatures above 500ºC, they observed a significant increase reaching a maximum of 0.77% at 800ºC. The increase in the number of voids inside the rock due to the increase in temperature also results in a decrease in the P-wave velocities and elastic parameters. This behavior is well documented e.g. [3], [10], [21], [23], [27]. Brotons et al. [21] who concluded that the decrease in the P-waves velocities is related to the increase in porosity as a consequence of the exposure of the limestone samples to high temperatures. The authors noted that the decrease in the P-waves velocities was more significant after reaching 300ºC. Martinho et al. [10] and Meng et al. [27] associated the decrease in the P-wave velocity with the formation of new cracks and the expansion of minerals, namely, calcite. Since the P-wave velocity is highly dependent on the presence of microcracks [18] and these increase with increasing temperature (causing an increase in open porosity) there was a need to relate these two parameters. In fact, the correlation between the decrease in the P-waves velocities and the increase in open porosity present was 94.38% showing a strong linear correlation.

Of the three modules studied (E, μ and K), the ones that suffered the greatest reduction with increasing temperature were the Young and shear modulus; and what suffered the least reduction was the bulk modulus. The reductions in elastic parameters with the increase in temperature are mainly related to the reduction in the propagation of P and S-waves velocities, which, in turn, is due to the increase in the open porosity and the water absorption capacity by capillary resulting from the creation and development of micro-cracks and chemical changes. Zhang et al. [8] found that Young's modulus decreased with increasing temperature and related this decrease to the creation and development of microcracks inside the rock. Martinho et al. [10] noted that the reduction in elastic parameters, due to heating, may be related to the initial porosity of the rock. The authors observed that the reduction in parameters is smaller for samples with higher initial porosity. From the values of Young's modulus and open porosity it is possible to verify that, for samples heated to 300ºC, the reduction of Young's modulus is greater for samples with greater initial porosity regardless of the type of immersion. In fact, the decrease in Young's modulus and the increase in open porosity are highly correlated with a correlation coefficient of 93.19%.

The type of cooling influences the decrease in elastic parameters. Samples completely immersed in water showed greater reductions in these parameters, especially samples heated at 300ºC. However, in samples heated to 600ºC this difference is reduced. Brotons et al. [21] observed the same behavior. These authors found that for temperatures up to 200ºC, the decrease in the modulus of elasticity was two times greater for the limestone samples cooled in water compared to the samples cooled to room temperature. However, the difference between Young's modulus values taking into account the cooling method is gradually reduced with increasing temperature. At 600ºC the reduction is 78% and 75% for samples cooled in water and at room temperature, respectively.

According to Telford et al.[28], the range of values of elastic parameters (E, K, and μ) that are normally found in rocks varies between 10 and 200 GPa, with Young's modulus being, in most cases, the largest elastic modulus and the shear modulus the smallest, that is, $E > K > \mu$. In the reference samples, all parameters are inserted within that range and the previously mentioned relationship. For samples heated to 300ºC, it is also verified that the elastic parameters are inserted within the range between 10 and 200 GPa, with the exception of the shear modulus in which values below 10 GPa were obtained. In contrast, for samples heated to 600ºC, all elastic parameters have values below 10 GPa. In heated samples, the order of greatness changes; K became greater than E, that is, $K > E > \mu$. This change in the order is due to the fact that the S-wave velocity undergoes a greater reduction with the increase in temperature compared to the P-wave velocity. This greater reduction in VS may be due to the fact that the S-wave propagate only in the solid matrix of the rock. Thus, the increase in open porosity with the increase in temperature may have contributed significantly to this reduction. This fact suggests that open porosity has a greater influence on the S-wave velocity than on the P-wave velocity. In fact, it was found that the correlation coefficient between the reduction of the S-wave velocity and the increase of open porosity is higher (0.9554) compared to the correlation coefficient between P-wave velocity and the increase in open porosity (0.9438).

The decrease in elastic parameters with increasing temperature is reflected in an increase in the Poisson's ratio. Since the mechanical strength of the rock decreases when subjected to high temperatures, due to the creation and expansion of cracks, and since the Poisson's ratio is higher for the most damaged rocks, it is expected that samples subjected to higher temperatures will have greater Poisson's ratio. In fact, Bieniawski, who studied the fracture mechanism in a rock material, concluded that the Poisson's ratio, which is constant during linear elastic deformation, increases due to the creation of new fractures or the propagation of existing fractures [29]. However, different results can be found in the literature e.g. [7], [10], [21], [30]. Koca et al. [30] observed, in marble samples, a significant decrease in the Poisson's ratio after reaching a temperature of 200ºC and concluded that this decrease was related to the disintegration of the samples. Zhang et al. [7], identified two different behaviors of the Poisson's ratio at two temperatures that they considered as “critical” temperatures in limestone samples. Below 200ºC, they observed an increase in the Poisson's ratio, which they justified as being an indication of

the good plasticity of the limestone under normal conditions. The second temperature, identified as critical temperature, was the temperature of 500ºC. After reaching this temperature, the authors observed a significant decrease in the Poisson's ratio. The authors used this decrease as an indication of the weakening of samples that became brittle. Martinho et al. [10] justified the decrease in the Poisson's ratio as a result of the proximity of the P and S wave velocity values.

The divergences in the results and in the interpretations of the values of the Poisson's ratio suggest that its evaluation has to be done critically. Since the Poisson's ratio was obtained dynamically, that is, using the P and S-waves velocities, they do not take into account the volumetric effect in which anisotropies and discontinuities have a great influence. This is proven by the fact that there was no founded a relationship between the increase in the Poisson's ratio and the increase in anisotropy, nor between the increase in the Poisson's ratio and the increase in open porosity. According to Gercek [31], the evaluation of the porosity involvement in the Poisson's ratio is complicated due to the intervention of the geometry, orientation, and size of the pores present inside the rock.

The tomograms with the 3D distribution of the P wave velocities show that this variety of Ançã limestones is quite heterogeneous (figures 4 to 9). With the increase in temperature, the distribution of velocities became more heterogeneous, which is justified by the increase in anisotropy that occurred in the heated samples resulting from the anisotropic thermal expansion of the calcite crystals.

5. Conclusion

The study carried out in this dissertation aimed to simulate the possible effects of fires (high temperatures) on the white-cream Ançã limestone. The evaluation of the possible effects was carried out by studying the change in some petrophysical properties of the stone for different test conditions. At the end of this dissertation, it is possible to affirm that the objective initially proposed was fulfilled, since it was possible to evaluate the degradation of the stone induced by the high temperatures through the analysis of the obtained tomograms. It was also possible to understand how high temperatures influence the petrophysical and elastic properties of this lithotype.

One of the forms of degradation induced by the action of elevated temperatures was the change of color on the surfaces of the heated samples. In the samples heated to 300ºC, the white color took on shades of beige cream and in the samples heated to 600ºC, the color became even darker taking with the samples to acquire shades of dark gray.

The increase in temperature also caused changes in the physical properties of the Ançã limestone. The results showed an increase in the water absorption coefficient by capillary and open porosity and a decrease in apparent density with increasing temperature. Regarding the elastic parameters, there was a decrease in all the elastic parameters studied (VP, VS, VP/VS, E, K, and μ) with the exception of the Poisson's coefficient in which a slight increase was observed.

The type of cooling (by total or partial immersion) had a significant influence on the different properties studied. For fully immersed samples, there was a greater increase in open porosity and a greater reduction in elastic parameters compared to partially immersed samples. The results obtained in the capillary tests were inconclusive since no significant differences were identified.

With increasing temperature, it was found that anisotropy also increased. This increase was more pronounced for samples heated to 600ºC, making it impossible to obtain tomograms for samples subjected to this temperature. For samples heated to 300ºC, it was found that the increase in anisotropy made the samples more heterogeneous.

References

[1] I. Maxwell, “Fire loss to historic buildings,” *Safeguarded Cult. Herit. Underst. & viability Enlarg. Eur. Proc. 7th Eur. Conf. “Saveur” 31st May-3rd June, 2006, Prague, Czech Repub.*, pp. 551–558, 2007.

[2] B. Chakrabarti, T. Yates, and A. Lewry, “Effect of fire damage on natural stonework in buildings,” *Constr. Build. Mater.*, vol. 10, no. 7, pp. 539–544, 1996, doi: 10.1016/0950-0618(95)00076-3.

[3] W. Zhang, H. Qian, Q. Sun, and Y. Chen, “Experimental study of the effect of high temperature on primary wave velocity and microstructure of limestone,” *Environ. Earth Sci.*, vol. 74, no. 7, pp. 5739–5748, 2015, doi: 10.1007/s12665-015-4591-4.

[4] G. Pia, L. Casnedi, and U. Sanna, “Pore size distribution influence on suction properties of calcareous stones in cultural heritage: Experimental data and model predictions,” *Adv. Mater. Sci. Eng.*, vol. 2016, 2016, doi: 10.1155/2016/7853156.

[5] X. Guo, G. Zou, Y. Wang, Y. Wang, and T. Gao, “Investigation of the temperature effect on rock permeability sensitivity,” *J. Pet. Sci. Eng.*, vol. 156, no. November 2016, pp. 616–622, 2017, doi: 10.1016/j.petrol.2017.06.045.

[6] A. Ozguven and Y. Ozcelik, “Investigation of some property changes of natural building stones exposed to fire and high heat,” *Constr. Build. Mater.*, vol. 38, pp. 813–821, 2013, doi: 10.1016/j.conbuildmat.2012.09.072.

[7] W. Zhang, Q. Sun, S. Zhu, and B. Wang, “Experimental study on mechanical and porous characteristics of limestone affected by high temperature,” *Appl. Therm. Eng.*, vol. 110, pp. 356–362, 2017, doi: 10.1016/j.applthermaleng.2016.08.194.

[8] J. Yang, L. Y. Fu, W. Zhang, and Z. Wang, “Mechanical property and thermal damage factor of limestone at high temperature,” *Int. J. Rock Mech. Min. Sci.*, vol. 117, no. March, pp. 11–19, 2019, doi: 10.1016/j.ijrmms.2019.03.012.

[9] A. Dionísio, M. A. Sequeira Braga, and J. C. Waerenborgh, “Fire induced colour modifications on limestones used as building materials in Portuguese monuments. A case study for built heritage,” *Limestone Charact. Compd. Appl.*, pp. 221–244, 2012.

[10] E. Martinho, M. Mendes, and A. Dionísio, “3D imaging of P-waves velocity as a tool for evaluation of heat induced limestone decay,” *Constr. Build. Mater.*, vol. 135, pp. 119–128, 2017, doi: 10.1016/j.conbuildmat.2016.12.192.

[11] J. Delgado Rodrigues, “As pedras de Coimbra. Aspectos relativos à sua degradação e conservação,” *Conf. Int. “A imagem dos centros históricos – bases para a sua salvaguarda”. Coimbra, Setembro 2005*, 2005.

[12] B. Trindade, M. F. Trindade, M. F. Ferreira, M. O. Q. Ferreira, M. O. Q. Oliveira, and R. Oliveira, "Contribution to the study of Ançã limestone Contribution to the study of Anca limestone," no. January, 2017.

[13] C. N. Costa and V. P. Silva, "Revisão histórica das curvas padronizadas de incêndio," *Nutau*, no. April 2020, 2006.

[14] EN 1925, "Natural stone test methods - Determination of water absorption coefficient by capillarity," *Standard*, 1999.

[15] "EN 1936 2001 Determinação das massas volúmicas real e aparente e das porosidades total e aberta" .

[16] M. Mendes, "A hybrid fast algorithm for first arrivals tomography," *Geophys. Prospect.*, vol. 57, no. 5, pp. 803–809, 2009, doi: 10.1111/j.1365-2478.2008.00755.x.

[17] F. Birch, "The Velocity of Compressional Waves in Rocks to 10 Kilobars, Part 1," vol. 65, pp. 1–20, 1961.

[18] A. M. Ferrero and P. Marini, "Technical note: Experimental studies on the mechanical behaviour of two thermal cracked marbles," *Rock Mech. Rock Eng.*, vol. 34, no. 1, pp. 57–66, 2001, doi: 10.1007/s006030170026.

[19] A. Ozguven and Y. Ozcelik, "Effects of high temperature on physico-mechanical properties of Turkish natural building stones," *Eng. Geol.*, vol. 183, pp. 127–136, 2014, doi: 10.1016/j.enggeo.2014.10.006.

[20] E. Franzoni, E. Sassoni, G. W. Scherer, and S. Naidu, "Artificial weathering of stone by heating," *J. Cult. Herit.*, vol. 14, no. 3 SUPPL, 2013, doi: 10.1016/j.culher.2012.11.026.

[21] V. Brotóns, R. Tomás, S. Ivorra, and J. C. Alarcón, "Temperature influence on the physical and mechanical properties of a porous rock: San Julian's calcarenite," *Eng. Geol.*, vol. 167, pp. 117–127, 2013, doi: 10.1016/j.enggeo.2013.10.012.

[22] M. Heidari, M. Torabi-Kaveh, and H. Mohseni, "Artificial weathering assessment of Persepolis stone due to heating to elucidate the effects of the burning of Persepolis," *Bull. Eng. Geol. Environ.*, vol. 75, no. 3, pp. 979–992, 2016, doi: 10.1007/s10064-016-0887-1.

[23] N. Sengun, "Influence of thermal damage on the physical and mechanical properties of carbonate rocks," *Arab. J. Geosci.*, vol. 7, no. 12, pp. 5543–5551, 2014, doi: 10.1007/s12517-013-1177-x.

[24] M. Gómez-Heras, M. A. De Buergo, R. Fort, M. Hajpál, A. Török, and M. J. Varas, "Evolution of porosity in Hungarian building stones after simulated burning," *Proc. Int. Conf. Heritage, Weather. Conserv. HWC 2006*, vol. 1, pp. 513–519, 2006.

[25] K. Beck, S. Janvier-Badosa, X. Brunetaud, Á. Török, and M. Al-Mukhtar, "Non-destructive diagnosis by colorimetry of building stone subjected to high temperatures," *Eur. J. Environ. Civ. Eng.*, vol. 20, no. 6, pp. 643–655, 2015, doi: 10.1080/19648189.2015.1035804.

[26] W. Zhang and C. Lv, "Effects of mineral content on limestone properties with exposure to different temperatures," *J. Pet. Sci. Eng.*, vol. 188, no. January, p. 106941, 2020, doi: 10.1016/j.petrol.2020.106941.

[27] Q. Bin Meng, C. K. Wang, J. F. Liu, M. W. Zhang, M. M. Lu, and Y. Wu, "Physical and micro-structural characteristics of limestone after high temperature exposure," *Bull. Eng. Geol. Environ.*, vol. 79, no. 3, pp. 1259–1274, 2020, doi: 10.1007/s10064-019-01620-0.

[28] L. P. G. and R. E. S. W.M. Telford, "Applied geophysics (second edition)," *Cambridge University Press*. 1991.

[29] R. Mech and G. Britain, "BIENIAWSKI National Mechanical Engineering Research Institute, Pretoria, South Africa," *Mech. Eng.*, vol. 4, no. c, p. 1967, 1967.

[30] M. Y. Koca, G. Ozden, A. B. Yavuz, C. Kincal, T. Onargan, and K. Kucuk, "Changes in the engineering properties of marble in fire-exposed columns," *Int. J. Rock Mech. Min. Sci.*, vol. 43, no. 4, pp. 520–530, 2006, doi: 10.1016/j.ijrmms.2005.09.007.

[31] H. Gercek, "Poisson's ratio values for rocks," *Int. J. Rock Mech. Min. Sci.*, vol. 44, no. 1, pp. 1–13, 2007, doi: 10.1016/j.ijrmms.2006.04.011.